Multimedia Tools and Applications
https://doi.org/10.1007/s11042-020-08769-x

Detection of myocardial infarction based on novel deep transfer learning methods for urban healthcare in smart cities

Ahmed Alghamdi[1] · Mohamed Hammad[2] · Hassan Ugail[3] · Asmaa Abdel-Raheem[4] · Khan Muhammad[5] · Hany S. Khalifa[6] · Ahmed A. Abd El-Latif[7,8,9]

Received: 4 October 2019 / Revised: 29 November 2019 / Accepted: 17 February 2020
Published online: 23 March 2020

Abstract
One of the common cardiac disorders is a cardiac attack called Myocardial infarction (MI), which occurs due to the blockage of one or more coronary arteries. Timely treatment of MI is important and slight delay results in severe consequences. Electrocardiogram (ECG) is the main diagnostic tool to monitor and reveal the MI signals. The complex nature of MI signals along with noise poses challenges to doctors for accurate and quick diagnosis. Manually studying large amounts of ECG data can be tedious and time-consuming. Therefore, there is a need for methods to automatically analyze the ECG data and make diagnosis. Number of studies has been presented to address MI detection, but most of these methods are computationally expensive and faces the problem of overfitting while dealing real data. In this paper, an effective computer-aided diagnosis (CAD) system is presented to detect MI signals using the convolution neural network (CNN) for urban healthcare in smart cities. Two types of transfer learning techniques are employed to retrain the pre-trained VGG-Net (Fine-tuning and VGG-Net as fixed feature extractor) and obtained two new networks VGG-MI1 and VGG-MI2. In the VGG-MI1 model, the last layer of the VGG-Net model is replaced with a specific layer according to our requirements and various functions are optimized to reduce overfitting. In the VGG-MI2 model, one layer of the VGG-Net model is selected as a feature descriptor of the ECG images to describe it with informative features. Considering the limited availability of dataset, ECG data is augmented which has increased the classification performance. A standard well-known database Physikalisch-Technische Bundesanstalt (PTB) Diagnostic ECG is used for the validation of the proposed framework. It is evident from experimental results that the proposed framework achieves a high accuracy surpasses the existing methods. In terms of accuracy, sensitivity, and specificity; VGG-MI1 achieved 99.02%, 98.76%, and 99.17%, respectively, while VGG-MI2 models achieved an accuracy of 99.22%, a sensitivity of 99.15%, and a specificity of 99.49%.

✉ Ahmed A. Abd El-Latif
a.rahiem@gmail.com

Extended author information available on the last page of the article

Keywords Deep learning · Myocardial infarction · ECG · Convolution neural network (CNN) · Smart cities

1 Introduction

Coronary heart disease, also known as ischemic heart disease, is the lead reason of deaths in the world, according to the World Health Organization (WHO). Over 17.7 million people die annually from cardiovascular diseases (CVDs), and over 70% of these deaths are due to heart attacks [8]. Partial or complete occlusion can cause inadequate blood flow toward coronary arteries, leading to the myocardial ischemia [15]. Myocardial Infarction (MI) is one of the common cardiac disorders caused by a prolonged myocardial ischemia and usually identified as a heart attack [28]. MI is a serious result of coronary artery disease. The heart functionality highly depends on the coronary circulation system that supplies oxygenated blood directly toward cardiac muscles to keep the heart nourished and oxygenated. MI occurs when a coronary artery is so severely blocked leading to the insufficient supply of nutrients and the oxygen-rich blood to a section of heart muscle. Sudden death occurs within an hour of the beginning indications of this disease [56]. Therefore, early detection of MI is important to prevent this heart condition from developing into a devastating fallout. Several methods including electrocardiogram (ECG), which is the most common medical tool that provides information about the waveform of the heartbeat can diagnose patients with MI. Other common diagnostic tests include magnetic resonance imaging (MRI) [57] and echocardiography [53]. However, the ECG is the first MI diagnostic method for urgent patients because it is easy to use and cost-effectively. Analyzing the MI signals manually is slightly hard because the nature of all the MI signals is not constant and noisy. Thus, numerous computer-aided diagnosis systems (CADs) have been proceeded to solve these difficulties. Nowadays, machine learning is a very common and effective tool to solve problems in the field of medicine [39, 40, 58], especially for MI detection [3, 5, 9, 12, 25, 31, 46, 54].

Several studies have been carried out to automate MI detection by analyzing ECG signals [3, 5, 9, 12, 25, 31, 46, 54]. Sadhukhan et al. [46] developed an automated ECG analysis algorithm based on the harmonic phase distribution pattern of the ECG data for MI identification. They yielded an average detection accuracy of 95.6% with a sensitivity of 96.5% and specificity of 92.7%. Jayachandran et al. [25] used the multi-resolution properties of wavelet transform to analyze the normal and MI ECG signals with an accuracy of 96.1%. Dohare et al. [12] detected the MI signals using 12-lead ECG data. They achieved a sensitivity of 96.66%, specificity of 96.66% and an accuracy of 96.66% with support vector machine (SVM) classifier. Arif et al. [5] implemented k-nearest neighbor (kNN) classifier and extracted time domain features of ECG beats to detect and localize the MI signals. They achieved a sensitivity of 99.97% and specificity of 99.9% for MI detection. However, in these studies [5, 12, 25, 46], the authors adopted on the classic machine learning approaches, which often suffer from overfitting and performance degradation when validated on a separate dataset. In this study, we did not follow these classical approaches, but build the proposed system with a convolutional neural network (CNN), which is one of the most widely used deep learning models. Recently, CNN has been utilized in the automated detection of abnormal heart conditions [21, 22, 41, 44, 51, 60, 62].

There are several approaches have been also proposed to detect MI by digital analysis of ECG signals [3, 9, 31, 54]. However, few of previous works based on CNN have been utilized for MI detection [2, 32, 61]. Wu et al. [61] employed deep feature learning and soft-max regression as a multi-class classifier for MI detection. They also incorporated multi-scale discrete wavelet transform into the feature learning process to increase the feature learning process. Their method yielded a sensitivity of 99.64% and specificity of 99.82%. Acharya et al. [2] detected the MI signals using an 11-layer 1-D CNN. They achieved an average accuracy of 95.22% using noise filters and 93.53% without using any noise filters. Liu et al. [32] proposed a method called multiple-feature-branch CNN (MFB-CNN) for MI detection with an accuracy of 98.79%. However, these works [2, 32, 61] used big convolution filters, which lead to increase the computation cost. Moreover, a few ECG segments were analyzed in most of these works and hence resulted in low specificity and sensitivity.

Following are the major shortcomings of these methods [2, 21, 22, 32, 41, 51, 60–62]:

- Utilizing very complex algorithms and costly in terms of MI detection.
- Sensitive to the quality of ECG signals.
- Work on multiple leads.
- Intensive to learn the features.
- Required big ECG data to get high performance.
- Obtain low-performance detection when working on other databases, which leads to overfitting.

Therefore, to overcome the previous limitations, this study proposes a novel deep learning approach for MI detection for deep urban healthcare in smart cities. The proposed method aims to achieve high classification accuracy than existing approaches, with following main goals:

- We propose a new deep model for MI detection to achieve high performance as compared to the previous detection techniques.
- Design a light-weight deep learning-assisted MI detection framework which is suitable for real-time ECG analysis.
- Building a model that working on a small number of ECG data with high performance.
- Developing a model that overcome the overfitting problem.

In this work, two ways of the transfer learning technique have been used [33]. The first way is fine-tuning the VGG-Net model and obtaining new network VGG-MI1. The second way is using the VGG-Net model as a feature extractor and obtaining new network VGG-MI2. Unlike most of the previous works, segmentation and feature extraction are no longer required in the proposed method. In addition, we optimized the proposed CNN model using data augmentation, which improve the accuracy of the proposed system by 2% in absolute values. Besides data augmentation, dropout technique is used [52] to avoid overfitting. The proposed algorithm is tested on the physikalisch-technische bundesanstalt (PTB) database [6] to evaluate its performance. The results obtained by our developed model show that the performance is better than existing algorithms based on CNN. The main contributions of this paper can be summarized below:

- A pre-trained deep CNN model is presented for MI detection, where we use VGG-Net that designed for the object recognition tasks to achieve state-of-the-art accuracy in MI detection. Also, we get a good representation of ECG data by selecting valuable layers as ECG features from VGG-Net.
- Unlike most of previous deep learning approaches, we employed small filter size in the first convolutional layers, which lead to lower computation cost and reduce noise effect. Moreover, we employ small number of pooling layers, which make the proposed two models more stable when using the input ECG image with size 128×128.
- We propose a method that work on the original ECG signals without using any signal filtering, which makes our method insensitive to the ECG signal quality.
- The proposed model is trained using only one ECG lead signal unlike most of previous algorithms. Hence, it reduces the computing cost and makes our method less complex than other previous methods.
- The robustness of the proposed system is increased against small variations by applying data augmentation techniques on the ECG data, which achieved high specificity and sensitivity in the results.
- We solve the small sample problem by employing a classifier called Q-Gaussian multi-class support vector machine (QG-MSVM), which lead to increase the accuracy of the proposed system.

The remainder of the paper is structured as follows: Section 2 gives the proposed myocardial infarction detection framework for urban healthcare in smart cities. In section 3, the proposed deep transfer learning method for the detection myocardial infarction is introduced. The dataset used for the experiments of the proposed approach is given in Section 4. Experimental analysis and results are given in Section 5. Section 6 reports and discusses the obtained results. Finally, Section 7 concludes this paper with future works.

2 The proposed myocardial infarction detection framework for urban healthcare in smart cities

Nowadays, computer vision equipped with modern technologies such as deep learning has the potential to demonstrate its possibilities beyond the law enforcement and surveillance purposes. From the autonomous vehicles to the interactive and intelligent architectures, groundbreaking applications open new ways to contribute to goals of smart cities concepts. These include a wide range of solutions in e-health care, intelligent transportation, surveillance, vehicle identification and tracking, smart parking, crowd density, and monitoring, etc. This paper aims to provide a platform to research community and professionals to demonstrate solutions and address research challenges in the development of detection of myocardial infarction using novel deep transfer learning methods for urban healthcare in smart cities.

Figure 1 shows the proposed myocardial infarction detection framework for urban healthcare in smart cities. The ECG signals are captured from medical sensors/devices in one side and send to the cloud-based E-healthcare for processing by the proposed deep transfer learning model in order to detect the myocardial infarction for patients. All the data are processing in urban healthcare in the smart city.

3 Methodology

In this study, the proposed method is validated on two ECG datasets with the same number of ECG beats. We used band-pass (Butterworth) filter with cutoff frequencies (0.5Hz and 40Hz) to remove the noise in one dataset. In the second dataset, we kept the noise in the ECG signals. After that, we carried out the peaks (P, R, and T) detection using our previous algorithm [18]. We defined a two ECG beats image using the detected peaks while excluding the first and the last ECG beat. Finally, the classification is performed with these obtained ECG images in CNN classification stage.

3.1 Preprocessing stage

In this stage, we plotted each ECG signal from the database and transformed it into two-dimensional gray-scale ECG image with size 128 × 128 [19, 27]. We are working on ECG as two-dimensional (2D) images as convolutional and max pooling layers of deep models are more appropriate for filtering the spatial locality of the ECG images, resulting in enhanced ECG classification. Furthermore, data augmentation methods can also play a role in boosting the accuracy by enriching the trained model with more complex and variant ECG content.

3.2 CNN classification stage

In this work, we adopted CNN to classify MI signals. CNNs are specialized versions of multilayer perceptron, with convolution operations instead of general matrix multiplications in

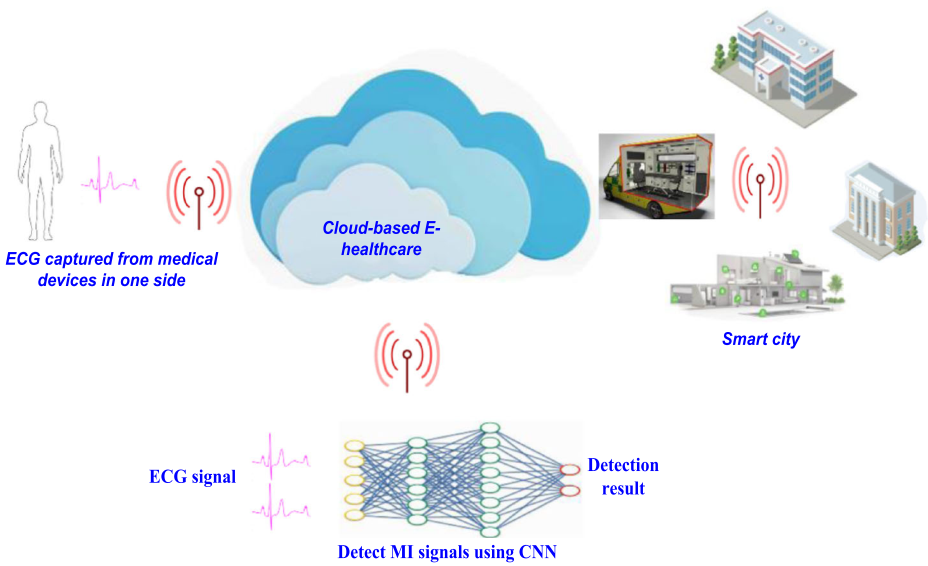

Fig. 1 The proposed myocardial infarction detection framework for urban healthcare in smart cities

the network layers [47]. CNNs have been broadly employed in numerous areas such as pattern recognition, image processing and other varieties of cognitive tasks [17, 20, 24, 42, 63]. Moreover, it is employed as an automated diagnostic tool in the medical fields [4, 23, 43]. A typical CNN includes an input layer, an output layer and various hidden layers, such as a convolutional (conv) layers, pooling (pool) layers and fully connected (full) layers. The convolutional layers are used for the detection of MI signal features. The pooling layers also called down-sampling layers used to control the overfitting and for reducing the weights number. The fully-connected layers used for classification.

3.2.1 Models

Large-scale image classification can be achieved with state-of-the-art CNN models such as Caffe-Net [26], Alex-Net [55], and VGG-Net [14]. In this study, we employed VGG-Net for classification due to its deeper architecture than other models [10]. In addition, the VGG-Net outperforms the other previous models. Finally, in the detection task of the ImageNet 2014 challenge, VGG-Net achieved the second place compared with other models [45].

3.2.2 The architecture of MI-CNN

VGG-Net is retrained to generate two new networks named VGG-MI1 and VGG-MI2. In both networks, the architecture of the VGG-Net is different from the standard VGG-Net by using small filter size in the first convolution layers and a small number of pooling layers, which lead to lower computation cost and makes the proposed models more stable for real-time ECG analysis. In addition to optimizing the standard VGG-Net, for VGG-MI1 we replaced the last 1000-entity from the SoftMax layer by a 2-unit SoftMax layer, which is initially intended to predict 1000 by a 2-unit soft-max layer (shown in Fig. 2), therefore the network can output the *two* classes (MI or normal) rather than the original 1000 classes that the network was designed for. In the second network VGG-MI2, we used the outputs of some selected layers as a feature descriptor of the input ECG image to describe it by useful and meaningful features and we

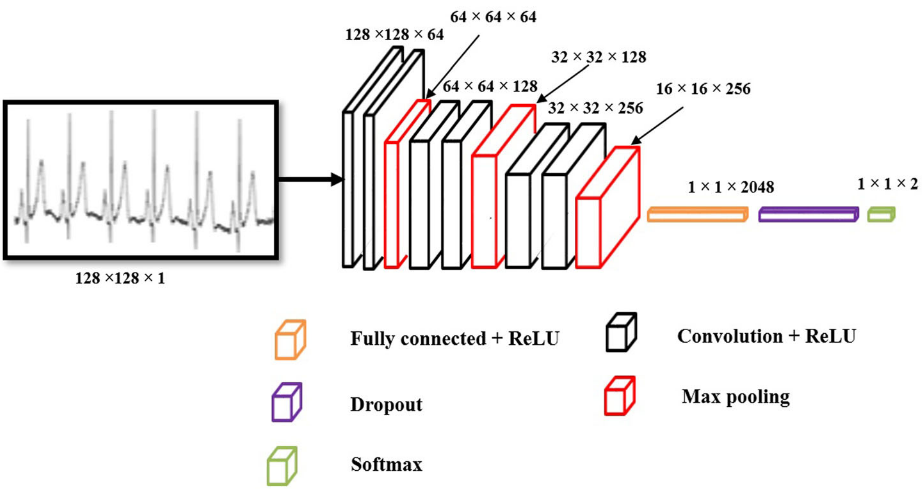

Fig. 2 The architecture of VGG-MI1

employed external classifier (QG-MSVM) for the classification to speed up the training task and improve the classification accuracy.

Table 1 shows the details of various layers of the proposed CNN network, which is six convolutional layers, *three* pooling layers followed by *two* fully connected layers and *one* soft-max layer, where the input images are resized to $128 \times 128 \times 1$. The pooling operation selects the maximum pooling strategy, which can achieve both dimensionality reduction and invariance. Since Local Response Normalization (LRN) leads to an increase in computing time and cost and does not affect the results, we did not employ it in the proposed model. We introduced non-linearity in the model by providing all layers with the Rectified Linear Unit (ReLU) activation function. In comparison with commonly used sigmoid and hyperbolic tan activation functions, ReLU does not saturate, thereby speeding up the convergence of stochastic gradient descent. The mathematical form of ReLU function is as follows:

$$f(x) = \max(0, x) \tag{1}$$

Where x is the input to a neuron. We employed 3×3 filters in the first convolutional layers to reduce the computing cost and the noise effect [29], which differs from most of the previous models that used large filters (e.g. 5×5 or 10×10 [35, 48]). The soft-max layer is the last layer of the network which is used to train the CNN. In this work, the dropout technique [52] is performed during the training phase with a probability of 0.5 and placed its position in the fully-connected layer to avoid overfitting. We do not apply a dropout to convolutional layers because they have a smaller number of parameters compared to the number of activations, which make the nodes not adaption together.

3.2.3 Optimized CNN architecture

We used two ways of the transfer learning technique [33] to retrain the VGG-Net and obtained two new networks VGG-MI1 and VGG-MI2. The two ways are as follows:

A. Replacing the last 1000-entity from the soft-max layer, which is initially intended to predict 1000 classes in VGG-Net model by a 2-unit soft-max layer, which assigns the two classes normal and MI. This network is called VGG-MI1 as shown in Fig. 2.

Table 1 The architecture of the proposed VGG-MI

Layers No.	Type	Kernel size	No. Kernels	Stride	Input size
Layer 1	Conv1	3×3	64	1	$128 \times 128 \times 1$
Layer 2	Conv2	3×3	64	1	$128 \times 128 \times 64$
Layer 3	Pool	2×2		2	$128 \times 128 \times 64$
Layer 4	Conv3	3×3	128	1	$64 \times 64 \times 64$
Layer 5	Conv4	3×3	128	1	$64 \times 64 \times 128$
Layer 6	Pool	2×2		2	$64 \times 64 \times 128$
Layer 7	Conv5	3×3	256	1	$32 \times 32 \times 128$
Layer 8	Conv6	3×3	256	1	$32 \times 32 \times 256$
Layer 9	Pool	2×2		2	$32 \times 32 \times 256$
Layer 10	Full		2048		$16 \times 16 \times 256$
Layer 11	Full		2048-dropout		2048
Layer 12	Soft		2		2048

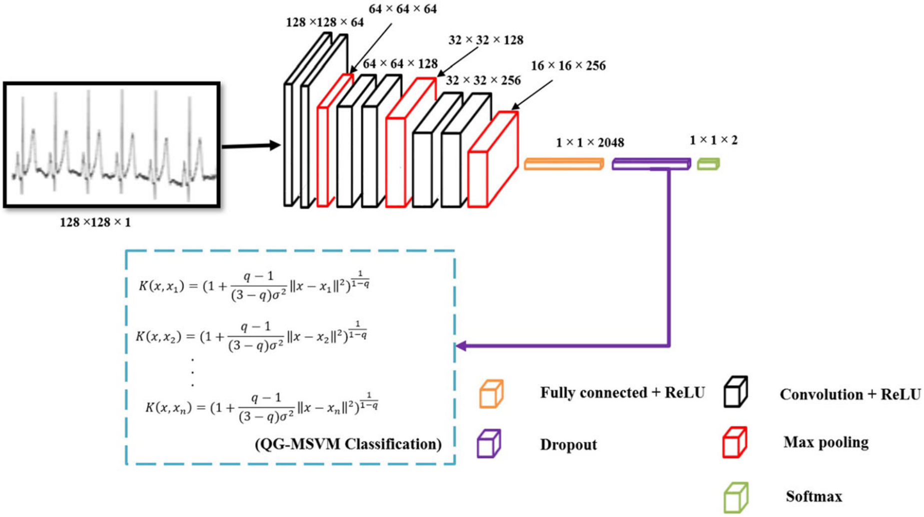

Fig. 3 The architecture of VGG-MI2

B. Selecting one layer as a feature descriptor of the training and test the ECG images to describe it with informative features. In our case, the second output fully connected layer is employed as a feature descriptor. This network is called VGG-MI2 as shown in Fig. 3.

For the VGG-MI1 model, besides replacing the last 1000-unit soft-max layer, we optimized various functions of the standard VGG-Net model to reduce overfitting and improve classification accuracy. For the VGG-MI2 model, second fully connected layer is selected to describe

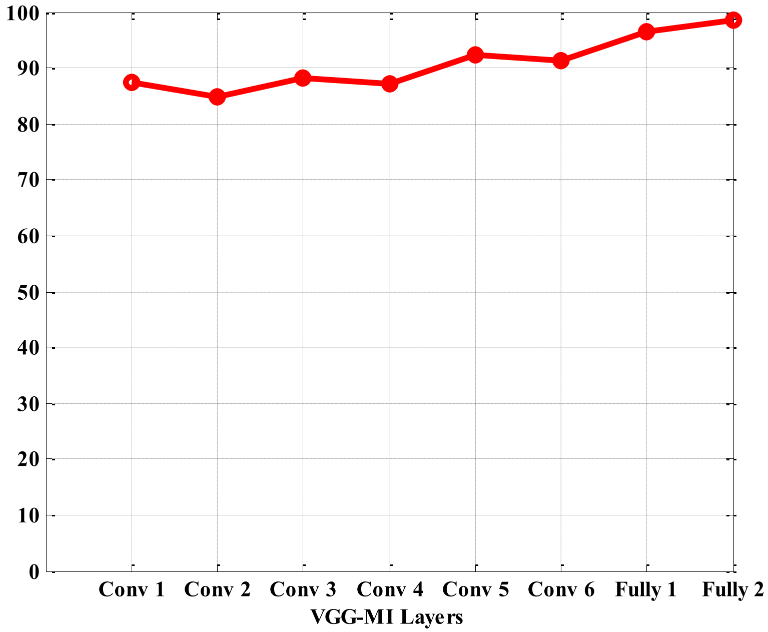

Fig. 4 Effect of the distinctive layer features on the classification accuracy

it with informative features because deeper layers contain higher-level features and also; we selected the layer that achieves the highest accuracy comparing to other layers in our model as shown in Fig. 4. Finally, the proposed models are compared with standard VGG-Net and Alex-Net.

3.2.4 Training

Stochastic gradient descent is used with momentum [7] for training the VGG-MI1 model with five samples for batch size. Gaussian distribution for random sampling with 10^{-2} standard deviation and *zero* mean is adopted for initializing the weights of the CNN filters. The hyper-parameters are set as follows: learning rate of 10^{-2}, weight decay of 5×10^{-4} and the training and testing of the CNN were done in 50 epochs. We changed these parameters iteratively accordingly to obtain optimum performance. Table 2 shows the configuration of the proposed CNN in this work.

The VGG-MI2 model was trained using Q-Gaussian multi-class support vector machine (QG-MSVM) classifier [16], which is defined as:

$$K(x, x_i) = \left(1 + \frac{q-1}{(3-q)\sigma^2}\|x-x_i\|^2\right)^{\frac{1}{1-q}} \tag{2}$$

Where q is a real-valued parameter, σ is a real value standard variance of Gaussian distribution and each $x_i \in R_p$ is a p-dimensional real vector. In our previous work [16], we used QG-MSVM to classify fingerprints, and we achieved a good result comparing to other SVM kernels. We modified the QG-MSVM to classify ECG. instead of classifying the fingerprint as in our previous work [16], which gives the best results compared to other SVM kernels: $\frac{1}{\sigma^2}$ is assigned to 0.5 and q to 1.5.

3.2.5 Testing

We perform a test on the CNN modal after every completed round of training epoch. The data were separated into *three* parts: 60%, 30% and 10% for training, validation and testing, respectively. Additionally, cross-validation method with ten-fold [13] is used. Finally, we evaluated the final performance of the system by calculating the average of all folds.

3.3 Data augmentation

In order to deal with the sparsely of data, and to enrich the trained model with more diverse, representatives and verities of data, various methods are used, and data augmentation is one of them. It makes the model more robust for overfitting. The augmentation technique is used in various fields and especially the medical field [11, 59]. In this study, data is augmented as: From each image of the dataset *nine* smaller images with 75% of each dimension of the original images are extracted: *four* images cropped from each corner, *one* at the center, *one* at the right center, *one* at the left center, *one* at the top center and *one* at the bottom center. After that, these augmented images are resized to the original image size 128 × 128. Hence, we created a database that is larger *ten* times than

Table 2 The most important VGG parameters

Parameter	Value
learning rate	0.001
standard deviation	0.01
mean	0
weight decay	0.0005
epochs	50
minibatch size	5 samples

the original one. Figure 5 shows the results (nine cropped images) after applying the augmentation technique on an original image.

4 Dataset

The PTB database [6] being a standard dataset in the MI detection was the natural choice for the validation of the proposed method. [2, 3, 5, 9, 12, 25, 31, 32, 46, 54, 61]. This database [6] contains 549 records from 290 subjects (*one* to *five* records per subject). Overall, the age range of the participants was between 17 and 87 (28% were female and 72% were male). There are *fifteen* measured signals in each record; the conventional 12-lead together with the *three* Frank lead ECG. The ECG signals are digitized at 1000 samples per second (1000 Hz). 147 out of 290 subjects and 368 out of 549 records are labelled as MI cases. In this work, we have used two-second duration of Lead II ECG signals with a total of 21,092 normal ECG beats and 80,364 MI ECG beats, where each two-beat represent a 128 × 128 Gray-scale image. Figure 6 shows an illustration of 2 s of normal and MI ECG signals with and without noise.

Fig. 5 Original ECG image and nine cropped images

5 Experimental results

The proposed algorithm is implemented in Matlab (R2017a on Microsoft Windows 10 Pro 64-bit). We used normal PC having 2.7-GHz CPU, 32GB RAM with GPU NVIDIA GeForce GTX 1080. The performance of the proposed fine-tuned models was compared with standard model of VGGNet and Alex-Net model. Moreover, a comparative analysis is performed with existing deep learning-based MI detection methods.

5.1 Performance metrics

Following standard metrics are used to assess the performance of the proposed algorithm:

1. The sensitivity (se) is defined as (3):

$$\mathrm{Se}(\%) = \frac{\mathrm{TP}}{\mathrm{FN} + \mathrm{TP}} \times 100 \tag{3}$$

2. The Predictivity (Pre) is defined as (4):

$$\mathrm{P}(\%) = \frac{\mathrm{TP}}{\mathrm{TP} + \mathrm{FP}} \times 100 \tag{4}$$

3. The Specificity (Spe) is defined as (5):

$$\mathrm{Spe}(\%) = \frac{\mathrm{TN}}{\mathrm{TN} + \mathrm{FP}} \times 100 \tag{5}$$

4. The Accuracy (Acc) is defined as (6):

$$\mathrm{Acc}(\%) = \frac{\mathrm{TP} + \mathrm{TN}}{\mathrm{TP} + \mathrm{FP} + \mathrm{FN}} \times 100 \tag{6}$$

where

The number of MI signals that classifies as normal is the False Negative (FN), False Positive (FP) denotes the number of normal ECG signals that classifies as MI, the number of

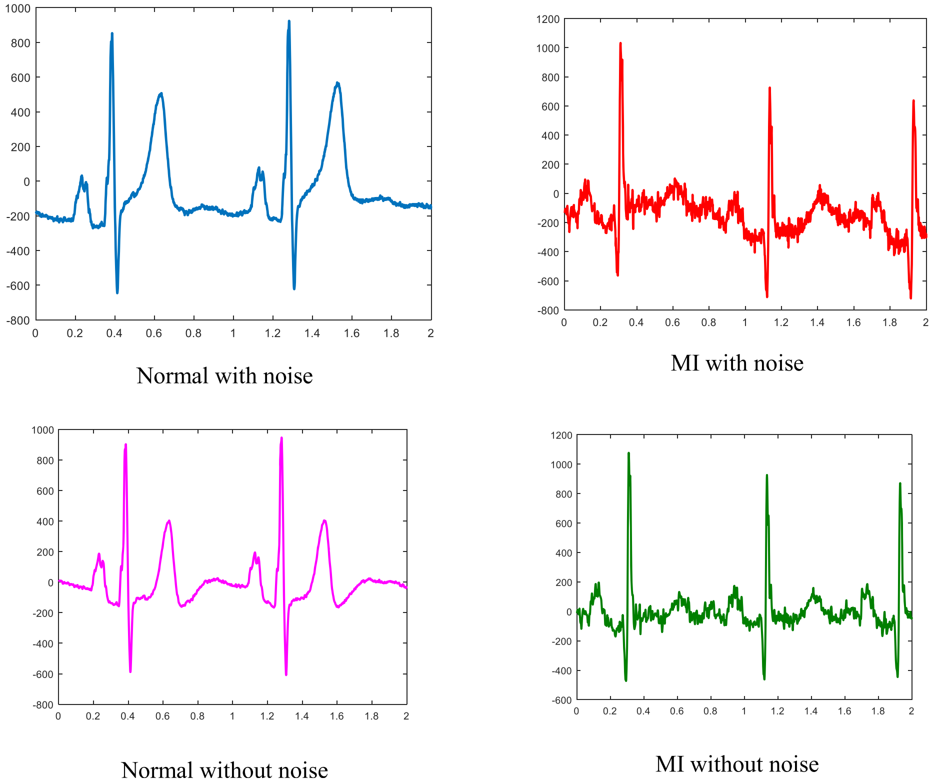

Fig. 6 Sample Normal and MI ECG signal with and without noise

normal ECG signals that classifies as normal is the True Negative (TN) and True Positive (TP) is the number of MI signals that classifies as MI.

5.2 Results

Four scenarios are used in this paper, the first scenario is the best-case1, in this case, we worked on MI signals without noise and we employed the augmentation technique on the trained data. The second scenario is the best-case2, in this case, we worked on MI signals without noise and without using augmentation technique. The third scenario is the worst-case1, in this case, we worked on MI signals with noise and using augmentation technique on the trained data. The last scenario is the worst-case2, in this case, we worked on MI signals with noise and without using augmentation technique. Acc, Se, Pre and Spe are calculated in all scenarios and the comparison is done between the proposed two models (VGG-MI1 and VGG-MI2) and the standard VGG-Net and Alex-Net on the PTB database.

The confusion matrix of the results for the two MI detection models with and without augmentation techniques across all folds is presented in Tables 3, 4, 5 and 6 respectively. It can be noted from the Table 3 that, 97.53% of ECG segments are correctly classified as Normal class, 96.95% of ECG segments are correctly classified as MI when using VGG-MI1 on ECG segments without noise and without augmentation technique and 99.17% of ECG segments are correctly classified as Normal class, 98.76% of ECG segments are correctly classified as

Table 3 Confusion matrix of ECG segments without noise across 10-fold for VGG-MI1

VGG-MI1	True/Predicted	Normal	MI	Acc (%)	Se (%)	Pre (%)	Spe (%)
Without augmentation	Normal	20,573	519	97.57	97.53	91.36	96.95
	MI	1945	78,419	97.57	96.95	99.34	97.53
With augmentation	Normal	209,174	1746	99.02	99.17	96.24	98.76
	MI	8168	795,472	99.02	98.76	99.78	99.17

MI when using augmentation technique. Also, in Table 4, 93.59% of ECG segments are correctly classified as Normal class, 92.53% of ECG segments are correctly classified as MI when using VGG-MI1 on ECG segments with noise and without augmentation technique and 94.83% of ECG segments are correctly classified as Normal class, and 95.46% of ECG segments are correctly classified as MI when using augmentation technique. For VGG-MI2, it can be noted from the Table 5 that, 98.53% of ECG segments are correctly classified as Normal class, 97.95% of ECG segments are correctly classified as MI when using VGG-MI2 on the second scenario (best-case2) and 99.49% of ECG segments are correctly classified as Normal class, 99.15% of ECG segments are correctly classified as MI when working on the first scenario (best-case1). Also, in Tables 6, 95.54% of ECG segments are correctly classified as Normal class, 95.08% of ECG segments are correctly classified as MI when using VGG-MI2 on the fourth scenario (worst-case2) and 96.79% of ECG segments are correctly classified as Normal class, and 97.35% of ECG segments are correctly classified as MI when working on the third scenario (worst-case1).

For VGG-MI1, a total of 2.4% Normal ECG segments are wrongly classified as MI and a total of 2.3% MI segments are wrongly classified as Normal without using augmentation technique after removing the noise. A total of 0.8% Normal ECG segments are wrongly classified as MI and a total of 1% MI segments are wrongly classified as Normal using augmentation technique after removing the noise.

For VGG-MI2, a total of 1.4% Normal ECG segments are wrongly classified as MI and a total of 2% MI segments are wrongly classified as Normal without using augmentation technique after removing the noise. A total of 0.5% Normal ECG segments are wrongly classified as MI and a total of 0.8% MI segments are wrongly classified as Normal using augmentation technique after removing the noise.

From previous Tables, we can show that the best results are obtained when using the first two scenarios (best-case1 and best-case2) so; we worked on these two scenarios in all comparisons in this paper.

The overall classification results for the proposed two MI detection models using the first and the second scenarios are collected in Tables 7 and 8.

Table 4 Confusion matrix of ECG segments with noise across 10-fold for VGG-MI1

VGG-MI1	True/Predicted	Normal	MI	Acc (%)	Se (%)	Pre (%)	Spe (%)
Without augmentation	Normal	19,744	1352	92.75	93.59	76.68	92.53
	MI	6003	74,361	92.75	92.53	98.21	93.59
With augmentation	Normal	200,031	10,889	95.33	94.83	84.59	95.46
	MI	36,421	767,219	95.33	95.46	98.60	94.83

Table 5 Confusion matrix of ECG segments without noise across 10-fold for VGG-MI2

VGG-MI2	True/Predicted	Normal	MI	Acc (%)	Se (%)	Pre (%)	Spe (%)
Without augmentation	Normal	20,783	309	98.07	98.53	92.68	97.95
	MI	1640	78,724	98.07	97.95	99.60	98.53
With augmentation	Normal	209,856	1064	99.22	99.49	96.84	99.15
	MI	6828	796,812	99.22	99.15	99.86	99.49

It can be seen from Tables 7 and 8 that: an accuracy of 99.02% and a sensitivity and specificity of 98.76% and 99.17% respectively are achieved using the first MI detection model (VGG-MI1) using augmentation after removing the noise. Also, an average accuracy, sensitivity, and specificity of 99.22%, 99.15%, and 99.49% respectively are obtained for the second MI detection model (VGG-MI2) using augmentation after removing the noise. The performance of the VGG-MI2 is better than the VGG-MI1 because we employed external classifier (the QG-MSVM classifier) in the VGG-MI2 model, which plays an important rule for increasing the accuracy of the proposed system. As well, QG-MSVM can solve the small sample problem that faces the CNN training, which usually requires large sample data. Thus, the performance of VGG-MI2 when using augmentation and without augmentation is better than VGG-MI1.

Table 9 summarizes a comparative study of the proposed two MI detection models with standard VGG-Net and Alex-Net.

6 Discussion

We have observed from Table 9 that the proposed two models after applying transfer learning techniques are shown the best accuracy, sensitivity, predictivity and specificity results when using the first scenario (without noise and with augmentation) comparing to other two models. For the second scenario (without noise and without augmentation), Alex-Net presents the best accuracy, sensitivity, predictivity and specificity results. The VGG-Net shows the worst results in both scenarios compared to other models, while the first proposed model VGG-MI1 shows the worst sensitivity results compared to the proposed second model VGG-MI2 and the other models. In the second scenario, the difference between the VGG-MI1 and the standard VGG-Net in the average sensitivity is 0.3%, which is a small difference, so we can consider that the sensitivity of the VGG-MI1 is acceptable compared to other models. In the first scenario, the discrimination between the VGG-MI1 and Alex-Net is 0.33% and between the VGG-MI2 and Alex-Net is 0.53%. In the second scenario, the discrimination between Alex-Net and the VGG-MI1 is 0.67% and between Alex-Net and the VGG-MI2 is 0.17%. Also, we have observed from Table 9 that there is a big gap in the performance between the proposed two

Table 6 Confusion matrix of ECG segments with noise across 10-fold for VGG-MI2

VGG-MI2	True/Predicted	Normal	MI	Acc (%)	Se (%)	Pre (%)	Spe (%)
Without augmentation	Normal	20,152	940	95.17	95.54	83.60	95.08
	MI	3951	76,413	95.17	95.08	98.78	95.54
With augmentation	Normal	204,170	6750	97.24	96.79	90.64	97.35
	MI	21,250	782,390	97.24	97.35	99.14	96.79

Table 7 The overall classification results for VGG-MI1 using the first and the second scenarios

VGG-MI1	TP	TN	FP	FN	Acc (%)	Se (%)	Pre (%)	Spe (%)
With Augmentation	795,472	209,174	1746	8168	99.02	98.76	99.78	99.17
Without Augmentation	78,149	20,573	519	1945	97.57	96.95	99.34	97.53

models and the VGG-Net model. The reason for this gap is that we employed two ways of the transfer learning technique, which updated the standard VGG-Net model by reducing the number of pooling layers in our models (we used 3 pooling layers instead of 4 layers). Moreover, in the VGG-MI2 model, we employed QG-MSVM classifier, which plays an important rule for increasing the accuracy of the proposed system. From Tables 7 and 8, we can show that the VGG-MI2 model achieved high accuracy than the VGG-MI1 model. In addition, data augmentation technique plays an important rule for increasing the specificity and the sensitivity rates for all models. Alex-Net gives the best performance in the second scenario (when applying it to a small number of ECG), however, the sensitivity and specificity for the VGG-MI2 in the second scenario are also acceptable comparing to this model. According to this, we intend in the future to apply the transfer learning technique on Alex-Net and observe the results on a small number of ECG segments.

We compared the proposed models with previous MI detection methods on the PTB database as shown in Table 10. Numerous studies have been applied for automated MI detection [1–3, 5, 9, 12, 18, 25, 30–32, 34, 46, 49, 50, 54, 61]. Sun et al. [54], proposed an automatic system for MI detection. They discussed the rationale for applying multiple instances learning (MIL) to automated ECG classification. They yielded a sensitivity of 92.30% and specificity of 88.10% using KNN ensemble as a classifier. Sharma et al. [49], proposed a technique based on multiscale energy and eigenspace (MEES) approach for the detection of MI. This method obtained an accuracy of 96%, a sensitivity of 93% and specificity of 99% using SVM as a classifier and an accuracy of 81%, a sensitivity of 85% and specificity of 77% using KNN as a classifier. Acharya et al. [1], proposed a method for automated detection of MI by using ECG signal analysis. They extracted 12 nonlinear features from a discrete wavelet transform (DWT) coefficients. They yielded an accuracy of 98.80%, a sensitivity of 99.45% and specificity of 96.27% using KNN as a classifier. Sadhukhan et al. [46], developed an automated ECG analysis algorithm for MI detection. They used harmonic phase values as features, and then they used Threshold-Based classifier for classification. They achieved accuracy, sensitivity and specificity rates of 91.10%, 93.60%, and 89.90% respectively. Sharma et al. [50], designed a two-band optimal biorthogonal filter bank (FB) for classification of the MI ECG signals using dataset without noise and noisy dataset. This method obtained an accuracy of 99.74% for the dataset without noise and an accuracy of 99.62% for the dataset with noise using KNN as a classifier. In addition, we updated our previous algorithm [18] to be suitable for MI detection by adding some conditions (according to the cardiologist) in the classification algorithm, such as: If Q-wave is more than 0.04 s and

Table 8 The overall classification results for VGG-MI2 using the first and the second scenarios

VGG-MI2	TP	TN	FP	FN	Acc (%)	Se (%)	Pre (%)	Spe (%)
With Augmentation	796,812	209,856	1064	6828	99.22	99.15	99.86	99.49
Without Augmentation	78,724	20,783	309	1640	98.07	97.95	99.60	98.53

Table 9 Summarizes evaluation results of the proposed models and other two models using the first and the second scenarios (the results for the proposed approaches are given in bold)

Model	Acc (%)	Se (%)	Pre (%)	Spe (%)
VGG-Net with Augmentation	97.35	97.44	99.20	97.02
VGG-Net without Augmentation	97.11	97.25	99.07	96.54
Alex-Net with Augmentation	98.69	98.63	99.67	98.77
Alex-Net without Augmentation	98.24	98.03	99.73	99.01
VGG-MI1 with Augmentation	**99.02**	**98.76**	**99.78**	**99.49**
VGG-MI1 without Augmentation	**97.57**	**96.95**	**99.34**	**97.53**
VGG-MI2 with Augmentation	**99.22**	**99.15**	**99.86**	**99.49**
VGG-MI2 without Augmentation	**98.07**	**97.95**	**99.60**	**98.53**

more than 25% of the size of the following R-wave the signal is MI. After applying all conditions to the classification algorithm, we achieved an accuracy of 96%, a sensitivity of 95.39% and specificity of 97.22%. Wu et al. [61], proposed a deep feature learning-based MI detection and classification approach. They employed SoftMax regressor to perform multiple-class classification with a sensitivity of 99.64% and specificity of 99.82%. Acharya et al. [2], implemented a CNN algorithm for the automated detection of MI signals. They used Pan Tompkins algorithm [37] for R-peak detection. They segmented the ECG signals and normalized it using Z-score normalization. Finally, they used 1-dimensional deep learning CNN for training and testing. They achieved the highest accuracy of 95.22% sensitivity of 95.49% and specificity of 94.19% when using noise filters.

It is evident from the analysis of the results that our proposed algorithm is more robust compared to other works that mentioned in Table 10. Most of the previous researches [3, 9, 31, 34, 49, 54] work on a small number of ECG segments, which gives a low sensitivity rate. In our study, we solved this problem by using data augmentation technique, which gives high specificity and sensitivity rates. Furthermore, the methods proposed in [1, 3, 5, 9, 12, 31, 46, 49, 54, 61] used ECG recordings of more than one lead, however, we used only lead II ECG signals, which makes our methods less complex than other methods that used more than one lead. Moreover, our methods achieved the highest accuracy comparing to the existing methods that are used CNN and mentioned in Table 10. In addition, we updated our previous work [18] to detect the MI signals, but it gives lower accuracy (96%) comparing to the proposed method. The reason for the low accuracy of our previous work is that this method is sensitive to the ECG signal quality and cannot detect the noisy MI signals correctly. However, the proposed method performed well for clear and noisy MI signals.

The advantages of our proposed algorithm are summarized below:

- Transfer learning is successfully employed to increase the robustness of the proposed models.
- The proposed method achieves superior results compared with the previous deep learning methods.
- Data augmentation plays an important rule to increase the robustness of the proposed system against small variations.
- Segmentation and feature extraction are no longer required in the proposed method.
- Using small filter size in the first convolution layers and a small number of pooling layers lead to lower computation cost and make the proposed models more stable when using the input ECG image.

Table 10 Summary of a comparative study of the proposed algorithm with selected well-known methods (the results for the proposed approach are given in **bold**)

Author	Year	Number of ECG beats	Approach	Performances (%)		
				Accuracy	Sensitivity	Specificity
Jayachandran et al. [25]	2009	Normal: 2,282 MI: 718	- DWT - Daubechies 6 wavelet	96.05	N/R	N/R
Arif et al. [5]	2010	Normal: 3,200 MI: 16,960	- Wavelet transforms - KNN	98.30	99.97	99.90
Al-Kindi et al. [3]	2011	40 records	- Digital signal analysis techniques - Clinical background	N/R	85	100
Sun et al. [54]	2012	Normal: 79 records MI: 369 records	- Multiple instance learning - KNN ensemble	N/R	92.3	88.1
Chang et al. [9]	2012	Normal: 547 MI: 582	- HMMs - GMMs	82.5	85.71	79.82
Liu et al. [31]	2014	Normal: 52 records MI: 148 records	- Polynomial function - DWT - J48 decision tree	94.4	N/R	N/R
Safdarian et al. [34]	2014	549 records	- Naive Bayes Classification	94.74	N/R	N/R
Sharma et al. [49]	2015	549 records	- Multiscale wavelet energies - Eigenvalues of multiscale covariance matrices - SVM - KNN	SVM: 96 KNN: 81	 93 85	 99 77
Wu et al. [61]	2016	10,000 samples	- MDFL	N/R	99.64	99.82
Acharya et al. [1]	2016	Normal: 125,652 MI: 485,753	- DWT - KNN	98.80	99.45	96.27
Kumar et al. [30]	2017	Normal: 10,546 MI: 40,182	- Daubechies 6 (db6) wavelet - FAWT - Sample Entropy - LS-SVM	99.31	N/R	N/R
Acharya et al. [2]	2017	Normal: 10,546 MI: 40,182	CNN	With noise: 93.53 Without noise 95.22	 93.71 95.49	 92.83 94.19
Hammad et al. [18]	2018	549 records	- Characteristics of ECG signals	96	95.39	97.22
Dohare et al. [12]	2018	120 records	- Principal Component Analysis - SVM	SVM:		

Table 10 (continued)

Author	Year	Number of ECG beats	Approach	Performances (%)		
				Accuracy	Sensitivity	Specificity
				98.33	96.96	100
				SVM with PCA:		
				96.66	96.96	96.96
Sharma et al. [50]	2018	Normal: 10,546 MI: 40,182	- Two-band optimal biorthogonal filter bank - KNN	Without noise:		
				99.74	99.84	99.35
				With noise:		
				99.62	99.76	99.12
Liu et al. [32]	2018	MI: 13,577 Normal: 3,135	CNN	With noise:		
				98.59	99.79	97.44
				Without noise:		
				99.34	99.79	94.50
Sadhukhan et al. [46]	2018	MI: 15,000 Normal: 5,000	- Harmonic phase distribution pattern - Threshold-Based Classifier - Logistic Regression (LR)	Threshold:		
				91.1	93.6	89.9
				LR:		
				95.6	96.5	92.7
Proposed	**2019**	**Normal: 21,092** **MI: 80,364**	**- CNN** **- QG-MSVM**	**VGG-MI1**		
				99.02	**98.79**	**99.49**
				VGG-MI2		
				99.22	**99.15**	**99.49**

*N/R: Not Reported

**DWT* Discrete Wavelet Transform, *KNN* K-Nearest Neighbor, *HMMs* hidden Markov models, *GMMs* Gaussian mixture models, *SVM* Support Vector Machine, *DFL* deep feature learning, *FAWT* flexible analytic wavelet transform, *LS-SVM* least-squares support vector machine, *CNN* Convolution Neural Network, *QG-MSVM* Q-Gaussian multi-class support vector machine

- Using QG-MSVM classifier lead to solve the small sample problem that faces the CNN training, which usually requires a large sample data.
- The real-time MI signals analysis with good accuracy makes the proposed method a suitable tool to be deployed in hospitals.

The disadvantages of the proposed work are as follows:

- The proposed algorithm is costly compute comparing to machine learning algorithms.
- Need to test more data using the proposed model.

7 Conclusion and future work

A computer-aided MI diagnostic system is presented for both rural and urban healthcare centers. Two transfer-learning techniques have been employed to fine-tune the pre-trained VGG-Net and generate two new tuned-models called VGG-MI1 and VGGMI2. Fine-tuning is based on the enhancement of the standard VGG architecture. Besides, we employed data augmentation technique to increase the classification accuracy. Two seconds ECG signals have been utilized from the PTB database to evaluate the effectiveness of the proposed method four different scenarios. Experimental results show that the best result is obtained when using the first scenario (best-case1) on the second model which is more accurate and robust compared to other previous works. We have achieved an accuracy of 99.22%, a sensitivity of 99.15% and specificity of 99.49% when using the best scenario on VGG-MI2. Also, we have achieved an accuracy of 97.24%, a sensitivity of 97.13% and specificity of 96.53% when using the worst scenario on VGG-MI2. This suggests that the proposed method can detect the MI signals with high-performance results even though there are noise present in the ECG beats. Hence, it is obvious that the proposed algorithm has the possibility to accurately diagnose MI signals and considered deploying in hospitals and clinics.

In the future, we aim to enhance our method to detect different types of heart diseases such as atrial fibrillation (A-Fib), ventricular fibrillation (V-Fib) and atrial flutter (AF). Also, we intend to use more augmentation types to improve the performance of our method. In addition, we attend to apply the proposed algorithm on different physiological signals such as electroencephalogram (EEG) [36, 38] and observe the effect of using our model on the EEG performance. Finally, we intend to apply other models on the MI data and observe the effect of these models on MI detection results.

Acknowledgments This project was funded by University of Jeddah, Jeddah, Saudi Arabia (Project number: UJ-02-018-ICGR). The authors, therefore, gratefully acknowledge DSR technical and financial support. Also, Ahmed A. Abd El-Latif acknowledges support from TYSP-Talented Young Scientist Program (China) and Menoufia University (Egypt). Additionally, the authors warmly thank their families for their unconditional support.

References

1. Acharya UR, Fujita H, Sudarshan VK, Shu LO, Adam M, Koh JEW et al (2016) Automated detection and localization of myocardial infarction using electrocardiogram: a comparative study of different leads. Knowl-Based Syst 99:146–156

2. Acharya UR, Fujita H, Lih OS, Hagiwara Y, Tan JH, Adam M (2017) Application of deep convolutional neural network for automated detection of myocardial infarction using ECG signals. Inf Sci 415-416:190–198
3. Al-Kindi SG, Ali F, Farghaly A, Nathani M, Tafreshi R (2011) Towards real-time detection of myocardial infarction by digital analysis of electrocardiograms. IEEE, 1st Middle East Conference on Biomedical Engineering, p.454–457
4. Amrani M, Hammad M, Jiang F, Wang K, Amrani A (2018) Very deep feature extraction and fusion for arrhythmias detection. Neural Comput Applic 30(7):2047–2057
5. Arif M, Malagore IA, Afsar FA (2012) Detection and localization of myocardial infarction using k-nearest neighbor classifier. J Med Syst 36(1):279–289
6. Bousseljot R, Kreiseler D, Schnabel, A (1995) Nutzung der EKG-Signaldatenbank CARDIODAT der PTB über das Internet. Biomedizinische Technik, Band 40, Ergänzungsband 1 S 317
7. Bouvrie J (2007) Notes on convolutional neural network
8. Cardiovascular disease, "World Heart Day" (2019) [Online]. Available: http://www.who.int/cardiovascular_diseases/world-heart-day/en/. Accessed: 30-Jan-2019.
9. Chang PC, Lin JJ, Hsieh JC, Weng J (2012) Myocardial infarction classification with multi-lead ECG using hidden markov models and gaussian mixture models. Appl Soft Comput 12(10):3165–3175
10. Chatfield K, Simonyan K, Vedaldi A, Zisserman A (2014) Return of the devil in the details: Delving deep into convolutional nets. In Proc. British Mach Vis Conf (BMVC)
11. Dan C, Meier U, Schmidhuber J (2012) Multi-column deep neural networks for image classification. IEEE Comput Vis Pattern Recognit 157:3642–3649
12. Dohare AK, Kumar V, Kumar R (2018) Detection of myocardial infarction in 12 lead ECG using support vector machine. Appl Soft Comput 64:138–147
13. Duda RO, Hart PE, Stork DG (2001) Pattern Classification 2nd Edition. Pattern classification. John Wiley and Sons, New York, pp 55–88
14. Girshick R, Donahue J, Darrell T, Malik J (2014) Rich Feature Hierarchies for Accurate Object Detection and Semantic Segmentation. 2014 IEEE conference on computer vision and pattern recognition (CVPR). IEEE Comput Soc
15. Hall J (2010) Guyton and Hall textbook of medical physiology: enhanced E-book: Elsevier Health Sciences
16. Hammad M, Wang K (2017) Fingerprint classification based on a Q-Gaussian multiclass support vector machine. In: Proceedings of the 2017 international conference on biometrics engineering and application. ACM
17. Hammad M, Wang K (2019) Parallel score fusion of ECG and fingerprint for human authentication based on convolution neural network. Comput Secur 81:107–122
18. Hammad M, Maher A, Wang K, Jiang F, Amrani M (2018) Detection of abnormal heart conditions based on characteristics of ECG signals. Measurement 125:634–644
19. Hammad M, Liu Y, Wang K (2018) Multimodal biometric authentication systems using convolution neural network based on different level fusion of ECG and fingerprint. IEEE Access 99:1–1. https://doi.org/10.1109/ACCESS.2018.2886573 Available from: https://ieeexplore.ieee.org/document/8575133/
20. Hammad M, Zhang S, Wang K (2019) A novel two-dimensional ECG feature extraction and classification algorithm based on convolution neural network for human authentication. Futur Gener Comput Syst
21. Han C, & Shi L (2019). ML–ResNet: a novel network to detect and locate myocardial infarction using 12 leads ECG. Comput Methods Prog Biomed 105138.
22. Han C, Shi L (2019) Automated interpretable detection of myocardial infarction fusing energy entropy and morphological features. Comput Methods Prog Biomed 175:9–23
23. Havaei M, Davy A, Warde-Farley D, Biard A, Courville A, Bengio Y, Pal C, Jodoin PM, Larochelle H (2017) Brain tumor segmentation with deep neural networks. Med Image Anal 35:18–31
24. Janwe NJ, Bhoyar KK (2017) Multi-label semantic concept detection in videos using fusion of asymmetrically trained deep convolutional neural networks and foreground driven concept co-occurrence matrix. Appl Intell 48:2047
25. Jayachandran ES, Joseph KP, Acharya UR (2010) Analysis of myocardial infarction using discrete wavelet transform. J Med Syst 34(6):985–992
26. Jia Y, Shelhamer E, Donahue J, Karayev S, Long J, Girshick R, Guadarrama S, Darrell T (2014) Caffe: Convolutional architecture for fast feature embedding. arXiv:1408.5093v1 [preprint]. [cited 2014 Jun 20]: [4 p.]. Available from: https://arxiv.org/abs/1408.5093
27. Jun TJ, Nguyen HM, Kang D, Kim D, Kim D, Kim YH (2018) ECG arrhythmia classification using a 2-d convolutional neural network. arXiv:1804.06812v1 [Preprint]. [cited 2018 Apr 18]: [22 p.]. Available from: https://arxiv.org/abs/1804.06812.
28. Kligfield P (2018) Goldberger's clinical electrocardiography: a simplified approach, Ary L. Goldberger, Zachary D. Goldberger, Alexei Shvilkin. J Electrocardiol 51(4):620

29. Krizhevsky A, Sutskever I, Hinton GE (2012) ImageNet classification with deep convolutional neural networks. Int Conf Neural Inf Proc Syst 60:1097–1105 Curran Associates Inc
30. Kumar M, Pachori RB, Acharya UR (2017) Automated diagnosis of myocardial infarction ECG signals using sample entropy in flexible analytic wavelet transform framework. Entropy 19(9):488. https://doi.org/10.3390/e19090488
31. Liu B, Liu J, Wang G, Huang K, Li F, Zheng Y, Luo Y, Zhou F (2015) A novel electrocardiogram parameterization algorithm and its application in myocardial infarction detection. Comput Biol Med 61: 178–184
32. Liu W, Huang Q, Chang S, Wang H, He J (2018) Multiple-feature-branch convolutional neural network for myocardial infarction diagnosis using electrocardiogram. Biomed Signal Proc Control 45:22–32
33. MathWorks, “Get Started with Transfer Learning”, (2019) [Online]. Available: https://www.mathworks.com/help/deeplearning/examples/get-started-with-transferlearning.html. Accessed: 30 Jan 2019
34. Naser S, Dabanloo N, Attarodi G (2014) A new pattern recognition method for detection and localization of myocardial infarction using T-wave integral and Total integral as extracted features from one cycle of ECG signal. J Biomed Sci Eng 5(7):818–824
35. Nogueira RF, Lotufo RDA, Machado RC (2017) Fingerprint liveness detection using convolutional neural networks. IEEE Trans Inf Forensics Secur 11(6):1206–1213
36. Oh SL, Vicnesh J, Ciaccio EJ, Yuvaraj R, Acharya UR (2019) Deep convolutional neural network model for automated diagnosis of schizophrenia using EEG signals. Appl Sci 9(14):2870
37. Pan J, Tompkins WJ (1985) A real-time QRS detection algorithm. Biomed Eng IEEE Trans 32(3):230–236
38. Paul JK, Iype T, Dileep R, Hagiwara Y, Koh JW, Acharya UR (2019). Characterization of fibromyalgia using sleep EEG signals with nonlinear dynamical features. Comput Biol Med 103331
39. Pławiak P (2018) Novel genetic ensembles of classifiers applied to myocardium dysfunction recognition based on ECG signals. Swarm Evol Comput 39:192–208
40. Pławiak P (2018) Novel methodology of cardiac health recognition based on ECG signals and evolutionary-neural system. Expert Syst Appl 92:334–349
41. Pławiak P, Acharya UR (2019) Novel deep genetic ensemble of classifiers for arrhythmia detection using ECG signals. Neural Comput & Applic:1–25
42. Protopapadakis E, Voulodimos A, Doulamis A, Doulamis N, Stathaki T (2019) Automatic crack detection for tunnel inspection using deep learning and heuristic image post-processing. Appl Intell 49:2793–2806. https://doi.org/10.1007/s10489-018-01396-y
43. Raghavendra U, Fujita H, Bhandary SV, Gudigar A, Tan JH, Acharya UR (2018) Deep convolution neural network for accurate diagnosis of glaucoma using digital fundus images. Inf Sci 441:41–49
44. Rajput JS, Sharma M, Acharya UR (2019) Hypertension diagnosis index for discrimination of high-risk hypertension ECG signals using optimal orthogonal wavelet filter Bank. Int J Environ Res Public Health 16(21):4068
45. Russakovsky O, Deng J, Su H, Krause J, Satheesh S, Ma S et al (2015) Imagenet large scale visual recognition challenge. Int J Comput Vis 115(3):211–252
46. Sadhukhan D, Pal S, Mitra M (2018) Automated identification of myocardial infarction using harmonic phase distribution pattern of ECG data. IEEE Trans Instrum Meas 99:1–11
47. Schmidhuber J (2015) Deep learning in neural networks: an overview. Neural Netw 61:85–117
48. Sermanet P, Eigen D, Zhang X, Mathieu M, Fergus R, LeCun Y (2014) OverFeat: integrated recognition, localization and detection using convolutional networks. In: Proceedings of ICLR
49. Sharma LN, Tripathy RK, Dandapat S (2015) Multiscale energy and eigenspace approach to detection and localization of myocardial infarction. IEEE Trans Biomed Eng 62(7):1827–1837
50. Sharma M, Tan RS, Acharya UR (2018) A novel automated diagnostic system for classification of myocardial infarction ECG signals using an optimal biorthogonal filter bank. Comput Biol Med 102: 341–356
51. Sharma M, Singh S, Kumar A, San Tan R, Acharya UR (2019) Automated detection of shockable and non-shockable arrhythmia using novel wavelet-based ECG features. Comput Biol Med 115:103446
52. Srivastava N, Hinton G, Krizhevsky A, Sutskever I, Salakhutdinov R (2014) Dropout: a simple way to prevent neural networks from overfitting. J Mach Learn Res 15(1):1929–1958
53. Strom JB, Tanguturi VK, Nagueh SF, Klein AL, Manning WJ (2019) Demonstrating the value of outcomes in echocardiography: imaging-based registries in improving patient care. J Am Soc Echocardiogr
54. Sun L, Lu Y, Yang K, Li S (2012) ECG analysis using multiple instance learning for myocardial infarction detection. IEEE Trans Biomed Eng 59(12):3348–3356
55. Sun J, Cai X, Sun F, Zhang J (2016) Scene image classification method based on Alex-Net model. IEEE, 2016 3rd International Conference on Informative and Cybernetics for Computational Social Systems (ICCSS)

56. Thygesen K, Alpert JS, Jaffe AS, Simoons ML, Chaitman BR, White HD (2012) Third universal definition of myocardial infarction. Circulation. 126(16):2020–2035
57. Tsai DY, Kojima K (2005) Measurements of texture features of medical images and its application to computer-aided diagnosis in cardiomyopathy. Measurement. 37(3):284–292
58. Tuncer T, Dogan S, Pławiak P, Acharya UR (2019) Automated arrhythmia detection using novel hexadecimal local pattern and multilevel wavelet transform with ECG signals. Knowl.-Based Syst 104923
59. Velasco JM, Garnica O, Contador S, Lanchares J, Maqueda E, Botella M, et al. (2017) Data augmentation and evolutionary algorithms to improve the prediction of blood glucose levels in scarcity of training data. IEEE Congress on Evolutionary Computation (CEC)
60. Wang Z, Qian L, Han C, Shi L (2020) Application of multi-feature fusion and random forests to the automated detection of myocardial infarction. Cogn Syst Res 59:15–26
61. Wu JF, Bao YL, Chan SC, Wu HC, Zhang L, Wei XG (2017) Myocardial infarction detection and classification — A new multi-scale deep feature learning approach. IEEE Int Conf Digit Signal Proc 309–313
62. Yıldırım Ö, Pławiak P, Tan RS, Acharya UR (2018) Arrhythmia detection using deep convolutional neural network with long duration ECG signals. Comput Biol Med 102:411–420
63. Zeng K, Ding S, Jia W (2019) Single image super-resolution using a polymorphic parallel CNN. Appl Intell 49:292–300. https://doi.org/10.1007/s10489-018-1270-7

Affiliations

Ahmed Alghamdi[1] · Mohamed Hammad[2] · Hassan Ugail[3] · Asmaa Abdel-Raheem[4] · Khan Muhammad[5] · Hany S. Khalifa[6] · Ahmed A. Abd El-Latif[7,8,9]

[1] Department of Cybersecurity, College of Computer Science and Engineering, University of Jeddah, Jeddah, Saudi Arabia

[2] Information Technology Department, Faculty of Computers and Information, Menoufia University, Shibin el Kom, Egypt

[3] Centre for Visual Computing, University of Bradford, Bradford BD7 1DP, UK

[4] Public health and Community Medicine Department, Faculty of Medicine, Menoufia University, Shebin El-Koom, Egypt

[5] Intelligent Media Lab, Department of Software, Sejong University, Seoul, Republic of Korea

[6] Computer Science Department, Misr Higher Institute of Commerce and Computers, Mansoura, Egypt

[7] Mathematics and Computer Science Department, Faculty of Science, Menoufia University, Shebin El-Koom, Egypt

[8] School of Information Technology and Computer Science, Nile University, Giza, Egypt

[9] School of Computer Science and Technology, Harbin Institute of Technology, Harbin 150080, China